Journal of Applied Polymer Science

A highly active and selective β-nucleating agent for isotactic polypropylene and crystallization behavior of β-nucleated isotactic polypropylene under rapid cooling

Shicheng Zhao, Hanzhang Gong, Xin Yu, Zhong Xin, Shibao Sun, Shuai Zhou, Yaoqi Shi
Shanghai Key Laboratory of Multiphase Materials Chemical Engineering, Department of Product Engineering, East China University of Science and Technology, Shanghai 200237, People's Republic of China
Correspondence to: Z. Xin (E-mail: xzh@ecust.edu.cn)

ABSTRACT: Zinc adipate (Adi-Zn) was observed to be a highly active and selective β-nucleating agent for isotactic polypropylene (iPP). The effects of Adi-Zn on the mechanical properties and the β-crystals content of nucleated iPP were investigated. The impact strength of iPP nucleated with 0.2 wt % Adi-Zn was 1.8 times higher than that of neat iPP. In addition, wide-angle X-ray diffraction analysis indicated that the content of β-crystals in nucleated iPP (k_β value) reached 0.973 with 0.1 wt % Adi-Zn, indicating that Adi-Zn is a highly active and selective β-nucleating agent for iPP. Furthermore, fast scanning chip calorimetry (FSC) studies using cooling rates from 60 to 13,800 °C min^{-1} revealed that the formation of β-crystals significantly depended on the cooling rates. At cooling rates below 3000 °C min^{-1}, only β-crystals existed. However, at cooling rates above 6000 °C min^{-1}, β-crystals failed to form. Moreover, a lower critical crystallization temperature that corresponded to the generation of β-crystals was investigated using cooling-induced crystallization, and the results are in good agreement with those of a previous study. © 2016 Wiley Periodicals, Inc. J. Appl. Polym. Sci. **2016**, *133*, 43767.

KEYWORDS: crystallization; mechanical properties; polyolefins

Received 24 January 2016; accepted 4 April 2016
DOI: 10.1002/app.43767

INTRODUCTION

Over the past few decades, much attention has been focused on the preparation of the β-crystal form of isotactic polypropylene (β-iPP) under laboratory and industrial conditions. The structure, morphology, processing, properties and application of β-iPP have been extensively studied.[1–6] In comparison to the traditional α-form of iPP (α-iPP), β-iPP exhibits improved elongation at break and better impact resistance.[7–10] These unique performance characteristics of β-iPP, which are advantageous in many applications, justify the extensive basic and applied research efforts that have been focused on this material.

β-iPP can be produced in the presence of efficient, selective β-nucleating agents (β-NAs) under practical conditions. Many available β-NAs have been previously reported.[10–18] The first efficient β-NA was γ-quinacridone (Dye Permanent Red E3B), which was reported by Leugering.[13] A two-component β-NA (i.e., compounds of pimelic acid and calcium stearate) was introduced by Shi *et al.*[14] Additional compounds with more defined structure that were similarly efficient included calcium salts of pimelic and suberic acid, as reported by Varga *et al.*[15] These two β-NAs have been categorized as a class containing certain group IIA metal salts or their mixtures with some specific dicarboxylic acids.[7,17] *N*,*N*′-Dicyclohexyl-2,6-naphthalenedicarboxamide (NU 100) is also an efficient β-NA that was developed in the past decade.[18] Although these substances can act as β-NAs for iPP, only a few aromatic amide compounds, such as NU 100, have been marketed. Unfortunately, NU 100 is not a highly selective β-NA, and α-iPP is always formed in its presence.[19] Therefore, a highly active and selective β-NA for iPP is still required. In recent years, a novel group IIB salt of alicyclic dicarboxylic acid that acts as a β-NA was investigated in our laboratory.[10] In this study, we reported a novel IIB salt of aliphatic dicarboxylic acid (i.e., zinc adipate), which acts as a highly active and selective β-NA for iPP. Our results further enrich the family of IIB salts of dicarboxylic acid for use as β-NAs of iPP.

β-iPP is thermodynamically metastable, which has been reported by Varga in detail.[20] The formation of β-iPP strongly depends on the crystallization process, especially the cooling rate.[10,21–23] Both Varga and Wittmann attributed this

Additional Supporting Information may be found in the online version of this article.

"sensitivity" to the upper and lower critical temperature limit of the formation of β-iPP.[24,25] The upper critical temperature limit is around 140 °C,[24] and the lower limit is at 100–105 °C.[25] Therefore, the growth rate of the β-phase is higher than that of α-phase between 100 and 140 °C. When the temperature is higher than 140 °C or lower than 100 °C, $\beta\alpha$-growth transition will take place on the surface of a growing β-spherulite. Apparently, the content of β-iPP depends on the cooling rate. Therefore, the exploration of the dependence of the formation of β-iPP on the cooling rate under real processing conditions is technologically important and scientifically fascinating. Previous investigations have been extensively performed under laboratory conditions using standard differential scanning calorimetry (DSC).[21–23] However, operational processes occur much faster compared to typical laboratory rates. Therefore, achieving controlled, constant heating and cooling rates that are much higher than the typical rates of standard DSC instruments, which range from 10 to 100 °C min^{-1}, is experimentally challenging. Recent advances in chip fast scanning calorimetry (FSC) by Mettler-Toledo (e.g., the Flash DSC 1 calorimeter, introduced October 2010) may provide the ability to investigate crystallization and melting behavior under rapid cooling rates. In this approach, the cooling rate and heating rate can reach 240,000 °C min^{-1}.[26] Therefore, FSC is a powerful tool for investigating the crystallization and melting behaviors of polymers by mimicking realistic conditions.[27,28] However, to the best of our knowledge, the literature contains few studies that address the dependence of β-crystals on the cooling rates under rapid cooling and supercooling.[29]

In the current study, a novel highly active and selective β-NA for iPP [i.e., zinc adipate (Adi-Zn)] was prepared and its nucleation effects were investigated. Herein, we provide a detailed overview of the dependence of β-crystal nucleation induced by Adi-Zn and the crystallization peak temperature of iPP/Adi-Zn on cooling rates under rapid cooling from 60 to 13,800 °C min^{-1} using FSC.

EXPERIMENTAL

Materials

A commercial iPP (trade name T30S, $M_w = 45.1 \times 10^4$ g·mol $^{-1}$, $M_w/M_n = 3.51$) was kindly supplied by Jiujiang Petroleum Chemical (China), with a melt flow index of 2.9 g/10 min (230 °C/2.16 kg). Adipic acid and zinc oxide were of analytical reagent grade and were obtained from Shanghai Lingfeng Chemical Regent Co., Ltd. (China).

Synthesis of Zinc Adipate

Zinc adipate was synthesized from the reaction of zinc oxide (ZnO) with adipic acid via mechanical stirring (Scheme 1).[30,31] Adipic acid (0.35 mol) and fine powdery ZnO were fully mixed in a 1:1 molar ratio by grinding. Next, an appropriate amount of water was added, and a slurry was formed. The mixture was then reacted for 12 h at 80 °C. The product, which was a white precipitate, was collected by filtration, washed several times with hot water, and dried at 105 °C for 12 h. The yield of Adi-Zn was 93.2%. The structure, crystal morphology, and thermostability of Adi-Zn were characterized by Fourier transform infrared spectroscopy, scanning electron microscopy, and thermogravimetric analysis (see the Supporting Information). The results indicated that rectangular crystals of Adi-Zn were synthesized (Supporting Information Figures S1 and S2) and exhibited a weight loss of 1 wt % that began at 364 °C (Supporting Information Figure S3), indicating the high thermal stability of Adi-Zn (230 °C). These results are consistent with those previously reported in the literature.[30] The crystals of Adi-Zn were milled to a fine powder and then sieved through a 200 mesh sieve prior to use.

$$HOOC(CH_2)_4COOH + ZnO \xrightarrow[12h]{\text{water, 80 °C}} ZnOOC(CH_2)_4COO$$

Scheme 1. Synthetic route to zinc adipate.

Sample Preparation

The β-NA (Adi-Zn) and antioxidant (Irganox 1010 and 168, 0.1 wt % relative to the iPP powder, respectively) were mixed with the iPP powder. This sample was extruded using a co-rotating twin-screw extruder (SJSH-30, Nanjing Rubber and Plastics Machinery Plant, China) and a strand die and was subsequently pelletized. The extrusion temperature profile was set at 190, 200, 200 200, 200, 200, 195, and 185 °C from the feed zone to the die. The dry iPP/Adi-Zn pellets were injected into standard test specimens using an injection-molding machine (CJ-80E, Guangdong Zhende Plastics Machinery Plant, China). The injection temperature was set at 220 °C. The mold temperature was about 40 °C and the cooling time was 35 s. Standard dumbbell-shaped samples for tensile property test were produced according to ASTM D-638 (type I). The samples for flexural property test were rectangular and their dimensions were 127 × 12.7 × 3.2 mm^3 (ASTM D-790). Rectangular samples (63.5 × 12.7 × 6.4 mm^3) with "V" notch were produced according to ASTM D-256 for impact strength test. The β-NA (Adi-Zn) was added at concentrations of 0.025, 0.05, 0.1, 0.2, 0.4, 0.6, 0.8, and 1.0 wt %. The resulting nucleated iPP samples are referred to as iPP/0.025Adi-Zn, iPP/0.05Adi-Zn, iPP/0.1Adi-Zn, iPP/0.2Adi-Zn, iPP/0.4Adi-Zn, iPP/0.6Adi-Zn, iPP/0.8Adi-Zn, and iPP/1Adi-Zn, respectively. A neat iPP sample was prepared using the same method for comparison.

Wide-Angle X-ray Diffraction

The wide-angle X-ray diffraction (WAXD) patterns were acquired using a Rigaku D/max-2550 VB/PC apparatus (Japan) equipped with a Cu Kα ($\lambda = 1.54$ Å) radiation source, and the diffraction angles (2θ) were obtained within the range from 10 to 30° (8° min^{-1}).

The β-crystal content (f) was determined according to previously reported procedures[32] using the following relationship:

$$k_\beta = \frac{H_\beta(300)}{H_\beta(300) + H_\alpha(110) + H_\alpha(040) + H_\alpha(130)} \quad (1)$$

where k_β is the relative proportion of the β-crystal form (WAXD) and $H_{\Omega(hkl)}$ is the height of the (hkl) peak associated with phase Ω (α or β; always with respect to the amorphous halo).

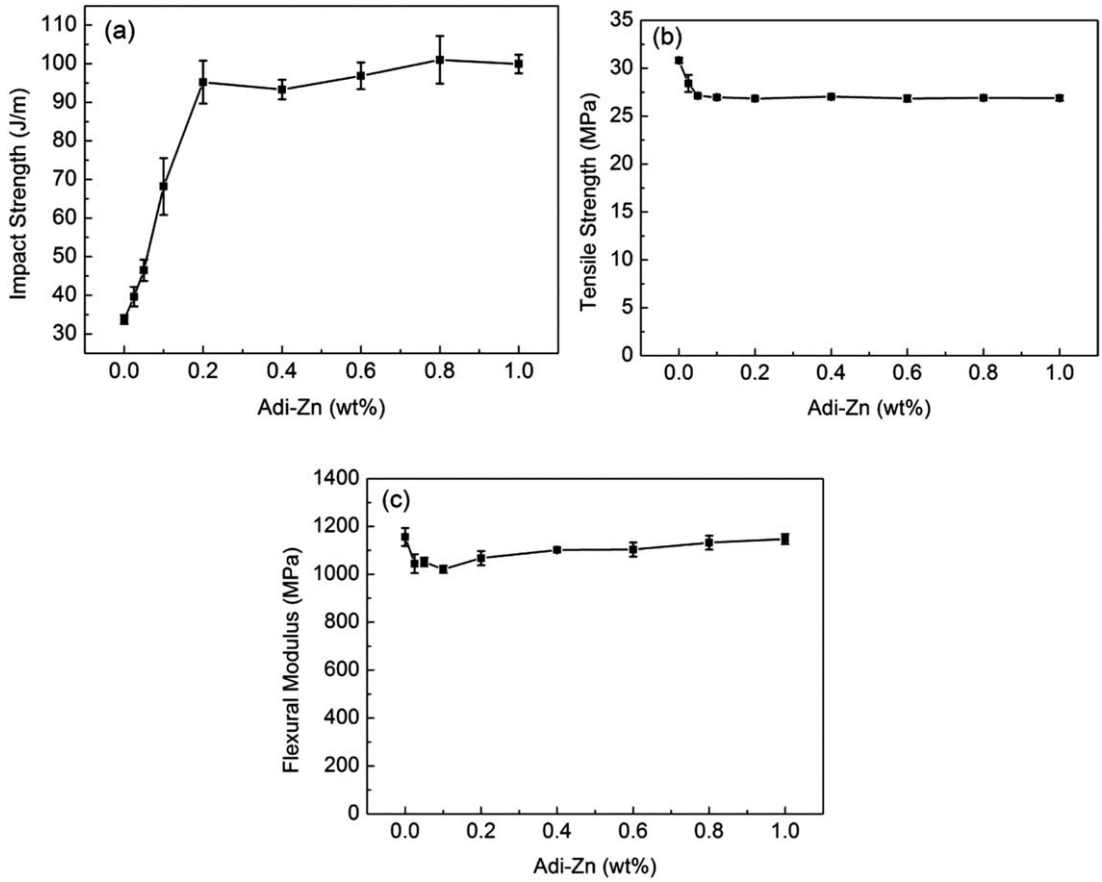

Figure 1. Mechanical properties of iPP nucleated with different Adi-Zn contents: (a) impact strength, (b) tensile strength and (c) flexural modulus.

Mechanical Properties

The mechanical properties were measured according to ASTM test methods, including D-638 for the tensile strength and D-790 for the flexural modulus, using a universal testing machine (MTS Systems Co., Ltd., Foshan City, China). The Izod impact strength was tested using standard method D-256 and an impact tester (MTS Systems Co., Ltd, Foshan City, China). The temperature of testing was room temperature (around 25 °C). The reported mechanical properties are the averaged of five independent measurements.

Polarized Optical Microscopy

The spherulitic morphologies of neat iPP and β-nucleated iPP were determined using polarized optical microscopy (POM) on an Olympus BX51 (Japan) that was equipped with a DP70 digital camera and a THMS600 hot-stage. The extruded samples were placed between two microscope slides, melted, pressed at 200 °C for 5 min to avoid possible self-nucleation of iPP; the samples were then cooled to 140 °C at a cooling rate of 100 °C min^{-1}. The samples were maintained under isothermal conditions until the crystallization process was completed, and the isothermal crystallization process was observed.

Differential Scanning Calorimetry

The crystallization and melting behavior of the samples were investigated using DSC (Diamond, Perkin-Elmer). The temperature was calibrated prior to the measurements using high-purity indium and zinc standards. The crystallization peak temperature (T_{cp}) was determined from the crystallization curves. All measurements were performed using 3-5 mg of sample at a standard heating and cooling rate of 10 °C min^{-1} under a nitrogen atmosphere from 50 to 200 °C; the samples were maintained at 200 °C for 5 min to release the thermal and mechanical history.

Fast Scanning Chip Calorimetry

FSC analyses of non-isothermal crystallization were performed with a power-compensation Mettler-Toledo Flash DSC 1 attached to a Huber TC100 intracooler. Small specimens were prepared using a microtome. The FSC sensor was conditioned and temperature-corrected according to the specifications of the instrument provider prior to the specimens being placed on the heatable area of the sample calorimeter. All of the samples were measured at a heating rate of 300 °C min^{-1} under a nitrogen atmosphere from 40 to 200 °C. The cooling rates during non-isothermal crystallization ranged from 60 to 13,800 °C min^{-1}. Additional details regarding the instrument and sensor have been reported elsewhere.[26,27]

RESULTS AND DISCUSSION

Mechanical Properties of iPP Nucleated with Adi-Zn

The macroscopic mechanical properties of iPP, especially its impact resistance, are strongly affected by the amount of β-NA. We, therefore, investigated the effect of the β-NA (Adi-Zn) content on the mechanical properties of iPP; the results are shown

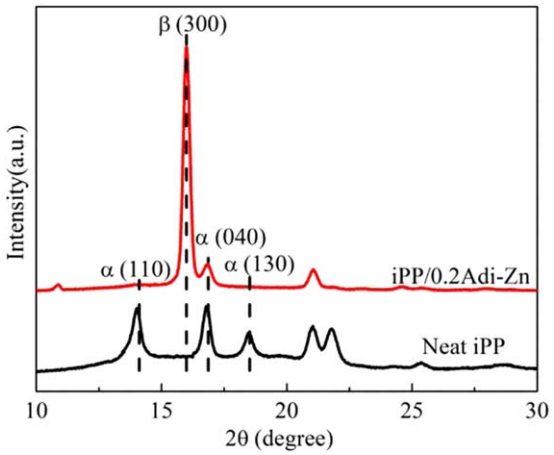

Figure 2. WAXD patterns of neat iPP and iPP/0.2Adi-Zn crystallized at 124°C under quiescent. [Color figure can be viewed in the online issue, which is available at wileyonlinelibrary.com.]

in Figure 1. As shown in Figure 1(a), the impact strength of nucleated iPP improved quickly when the loading of Adi-Zn was less than 0.2 wt % and then remained constant at higher Adi-Zn contents. When the content of Adi-Zn was 0.2 wt %, the impact strength of nucleated iPP increased nearly 1.8 times compared to that of neat iPP, indicating that Adi-Zn substantially improved the toughness of iPP. As shown in Figures 1(b,c), the tensile strength and flexural modulus of nucleated iPP gradually decreased and then remained constant with increasing Adi-Zn content. Therefore, the optimum Adi-Zn content for improving the impact resistance of iPP appears to be 0.2 wt %.

Effect of Adi-Zn on the β-Crystal Content of iPP

WAXD is a powerful tool for quantifying the β-crystal content of iPP. Figure 2 shows the WAXD patterns of neat iPP and iPP/0.2Adi-Zn crystallized at 124 °C under quiescent conditions. We chose a crystallization temperature of 124 °C on the basis of our analysis of the results from WAXD and DSC measurements of β-nucleated iPP samples crystallized at different temperatures (see Supporting Information Figures S4 and S5). In this profile, (110) at $2\theta = 14.1°$, (040) at 16.9°, and (130) at 18.5° were the principal reflections of the α-crystals of iPP, whereas (300) at approximately 16° was the principle reflection of the β-crystals. These reflections are considered marker peaks for the α- and β-crystals, respectively.

The variation in the k_β values as a function of the Adi-Zn concentration is shown in Figure 3. The results indicate that the k_β values increased sharply with the addition of Adi-Zn and that a maximum value of 0.973 was achieved when the concentration of Adi-Zn was 0.1 wt %. Thereafter, a slight decrease was observed with further increases in the Adi-Zn content. These results indicate that Adi-Zn is a highly active β-NA for iPP even at a very low loading concentration. In addition, Adi-Zn is a highly selective β-NA because the k_β values remain approximately 0.90 in the studied concentration range from 0.025 to 1 wt %. Notably, however, the saturation concentration of Adi-Zn determined from the mechanical properties and that determined from WAXD results differ, which may be due to the difference in the crystallization conditions of both measurements. Therefore, the effect of the crystallization condition on the β-crystal content needs to be investigated.

Dependence of the Formation of β-Crystals on the Cooling Rates

The formation of β-crystals depends on the concentration of the β-NA and the crystallization conditions, especially the cooling rates during crystallization.[29,33–35] Because FCS provided rapid cooling conditions that mimic crystallization in the practical processing of iPP, a variety of cooling rates from 60 to 13,800 °C min^{-1} as well as a heating rate of 300 °C min^{-1} were used in the current study. Selected FSC melting thermograms of neat iPP and iPP nucleated with 0.2 wt % Adi-Zn under different cooling rates are shown in Figure 4. For neat iPP, only one α-crystal melting peak was observed as the cooling rate increased. In contrast, crystallization of iPP induced by Adi-Zn exhibited a complex cooling rate dependence. When the cooling rate was less than 3000 °C min^{-1}, only a β-crystal melting peak was observed in Figure 4(b). At cooling rates greater than 3000 °C min^{-1}, the melting peak corresponding to α-crystals began to appear; the melting peak area of the β-crystals gradually decreased and nearly disappeared at cooling rates of 6000 °C min^{-1} and higher. Therefore, at cooling rates less than 3000 °C min^{-1}, β-crystals were predominant, at cooling rates between 3000 and 6000 °C min^{-1}, β-crystals and α-crystals coexisted, and at cooling rates higher than 6000 °C min^{-1}, α-crystals were predominant.

The dependence of the melting peak temperatures (T_{mp}) on the cooling rates was further plotted in Figure 5. The T_{mp} of neat iPP (black solid symbols) quickly decreased at the beginning and then plateaued with increasing cooling rates. A similar trend was observed for T_{mp} of β-crystals (red solid symbols) of iPP/0.2Adi-Zn. Interestingly, the T_{mp} of the α-crystals (blue open symbols) in iPP/0.2Adi-Zn is higher than that of neat iPP, which indicated that Adi-Zn triggered the formation of α-crystals rather than inducing β-crystal formation under rapid cooling and supercooling conditions. Therefore, the formation

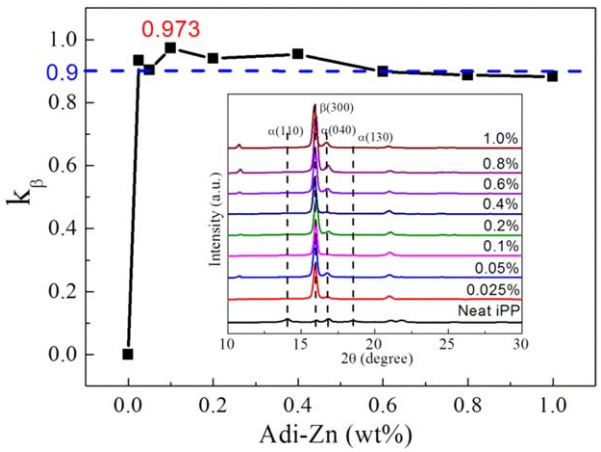

Figure 3. Values of kβ as a function of the Adi-Zn concentration. Inset: DSC thermograms of iPP with different amounts of Adi-Zn. [Color figure can be viewed in the online issue, which is available at wileyonlinelibrary.com.]

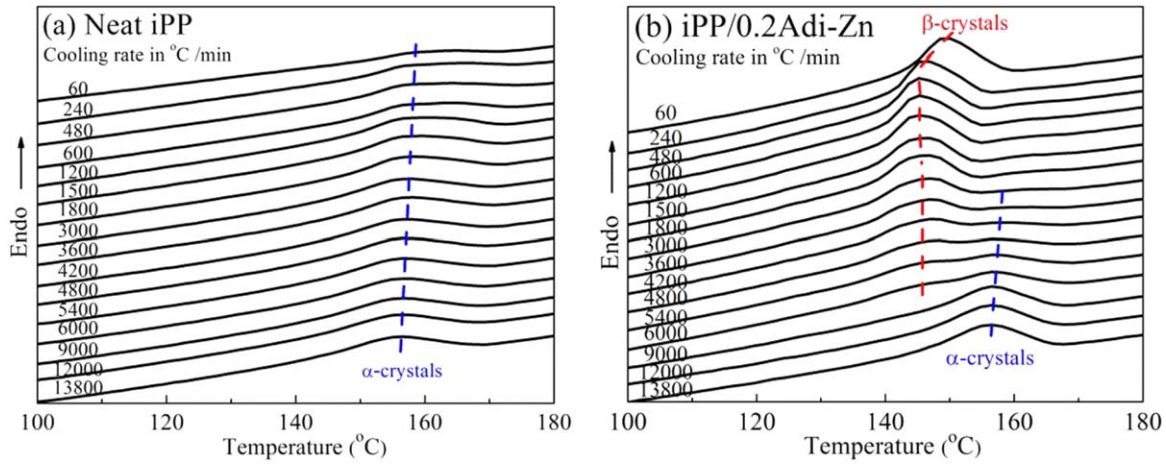

Figure 4. FSC heating curves of (a) neat iPP and (b) iPP/0.2Adi-Zn crystallizing under different supercooling conditions (heating rate: 300°C min^{-1}). [Color figure can be viewed in the online issue, which is available at wileyonlinelibrary.com.]

of β-crystals strongly depends on the cooling rate. These results provide a reasonable explanation for the difference in the saturation concentration of Adi-Zn obtained from the mechanical properties and WAXD results because the cooling rate of the former is much larger than that of the latter. The reason why the formation of β-crystals strongly depends on the cooling rate will be further discussed in the context of the crystallization process of iPP/Adi-Zn in Crystallization Behavior of β-Nucleated iPP under Rapid Cooling and Largely Different Supercooling section.

Crystallization Behavior of β-Nucleated iPP under Rapid Cooling and Largely Different Supercooling

The crystallization peak temperature (T_{cp}) of a polymer strongly depends on its cooling rate. The relationship between T_{cp} and the cooling rate has been previously studied by standard DSC. Because of the performance limitations of standard differential scanning calorimeters, the studied cooling rates reported in the literature typically cover a range from 1 to 100 °C min^{-1}. Heretofore, to the best of our knowledge, few publications have reported the dependence of T_{cp} on the cooling at higher cooling rates.[36] Therefore, we used FSC to study the effect of cooling rate on the T_{cp} values of neat iPP and nucleated iPP. The results may contribute to the optimization of industrial processing conditions.

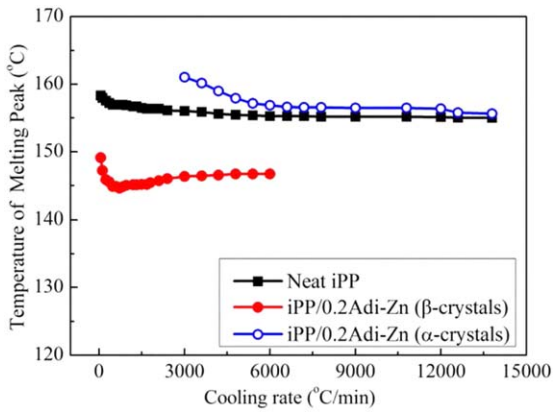

Figure 5. Dependence of the melting peak temperatures on the cooling rates. [Color figure can be viewed in the online issue, which is available at wileyonlinelibrary.com.]

The FSC cooling thermograms of neat iPP and iPP/0.2Adi-Zn are shown in Figure 6. According to the literature, the formation of β-crystals has a lower critical temperature limit ($T_c^{**} = 100$ °C) (i.e., β-crystals can be formed above T_c^{**}).[25,37] According to the results in Figure 6, at cooling rates less than 3000 °C min^{-1}, the overall crystallization occurred above T_c^{**}. Therefore, only β-crystals formed, as indicated in the corresponding melting curves [Figure 4(b)], marked with a red dotted line). At cooling rates higher than 6000 °C min^{-1}, the overall crystallization occurred below T_c^{**}. Therefore, only α-crystals were formed [Figure 4(b)], marked in blue dotted line). At cooling rates between 3000 °C min^{-1} and 6000 °C min^{-1}, partial crystallization occurred above T_c^{**}, which resulted in the coexistence of β- and α-crystals. These results provide a reasonable explanation for the dependence of the formation of β-crystals on the cooling rate under rapid cooling and supercooling conditions.

A detailed overview of the crystallization peak temperature of neat iPP and iPP/0.2Adi-Zn at different cooling rates is provided in Figure 7. The T_{cp} of the two samples gradually decreased with increasing cooling rates; the difference in their T_{cp} values (ΔT_{cp}) gradually increased until the cooling rate was approximately 3000 °C min^{-1} and then gradually decreased to nearly zero at a cooling rate of 13,800 °C min^{-1}. The maximum ΔT_{cp} values corresponded to cooling rates of approximately 3000 °C min^{-1}. The results revealed that heterogeneous nucleation (athermal nucleation) played a leading role in accelerating the crystallization of iPP below the critical cooling rate. In addition, homogeneous nucleation (thermal nucleation) played an increasingly important role at cooling rates above the critical cooling rate in β-nucleated iPP. When the cooling rate was 13,800 °C min^{-1}, Adi-Zn did not affect nucleation and could not accelerate the crystallization of iPP.

In addition, although Adi-Zn did not induce the formation of β-crystals when the cooling rate exceeded 6000 °C min^{-1}, the crystallization peak temperature of iPP/0.2Adi-Zn was still

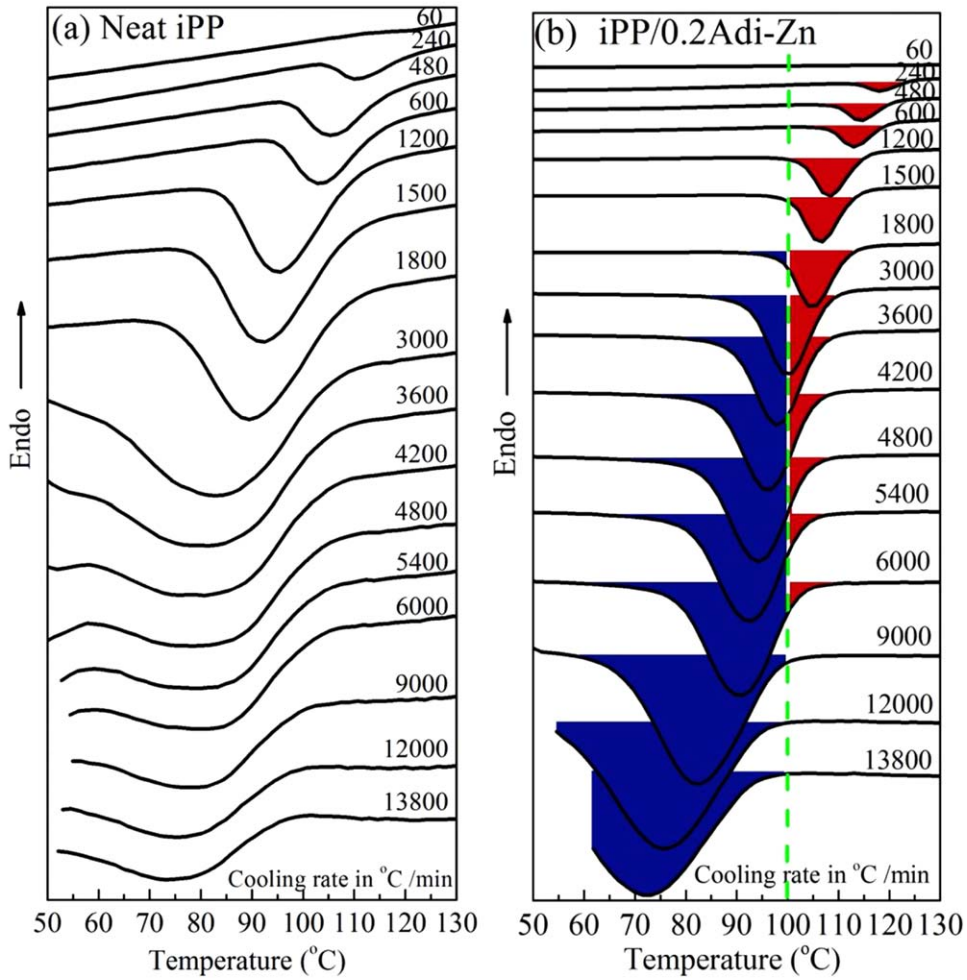

Figure 6. FSC scans for cooling of samples consisting of neat iPP (a) and iPP/0.2Adi-Zn (b) at different cooling rates. [Color figure can be viewed in the online issue, which is available at wileyonlinelibrary.com.]

higher than that of neat iPP, which confirmed that Adi-Zn acted as an α-NA under rapid cooling conditions. This observation is consistent with the previously noted increase in the melting peak temperature of iPP/0.2Adi-Zn compared to that of neat iPP under supercooling conditions, as shown in Figure 5.

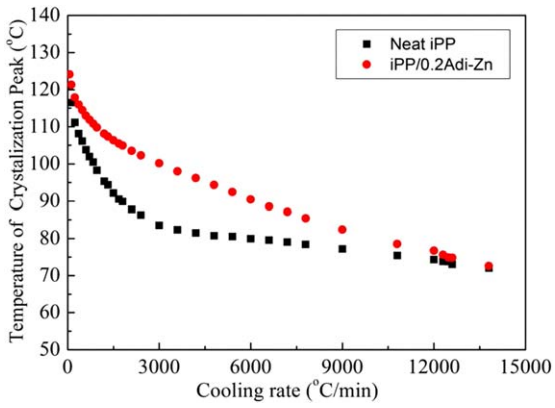

Figure 7. Dependence of the crystallization peak temperatures on the cooling rates. [Color figure can be viewed in the online issue, which is available at wileyonlinelibrary.com.]

Crystallization Behavior and Morphologies of iPP with Different Amounts of Adi-Zn

The dependence of the crystallization peak temperature (T_{cp}) of nucleated iPP on NA concentration has been previously investigated.[10,38] This type of study could contribute to an evaluation

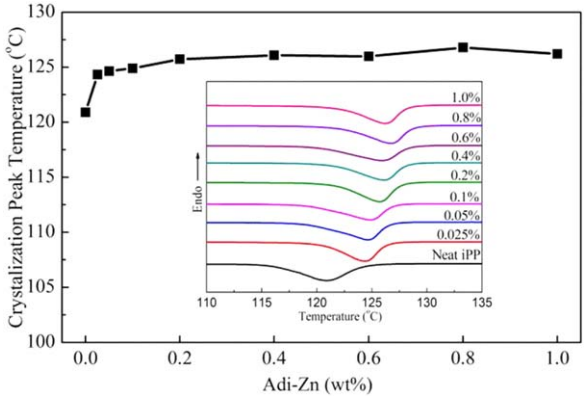

Figure 8. Dependence of the crystallization peak temperatures on the Adi-Zn content. Inset: DSC scans for samples with different Adi-Zn contents (cooling rate: 10 °C min^{-1}). [Color figure can be viewed in the online issue, which is available at wileyonlinelibrary.com.]

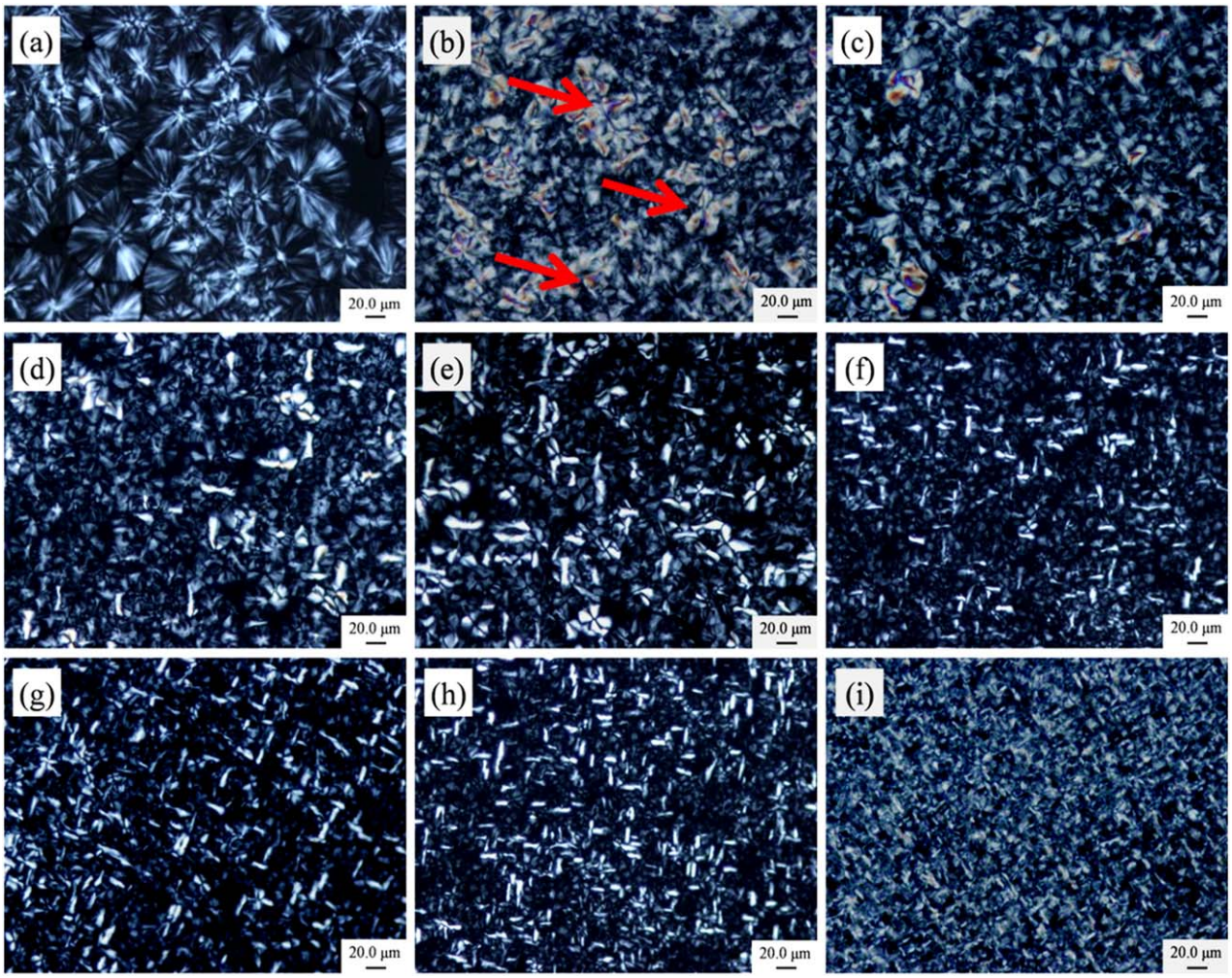

Figure 9. Polarized optical microphotographs of iPP samples crystallized at 140 °C: (a) neat iPP, (b) iPP/0.025Adi-Zn, (c) iPP/0.05Adi-Zn, (d) iPP/0.1Adi-Zn, (e) iPP/0.2Adi-Zn, (f) iPP/0.4Adi-Zn, (g) iPP/0.6Adi-Zn, (h) iPP/0.8Adi-Zn and (i) iPP/1Adi-Zn. [Color figure can be viewed in the online issue, which is available at wileyonlinelibrary.com.]

of the nucleating efficiency and to optimization of the processing conditions. Standard DSC was used to study the non-isothermal crystallization behavior of neat iPP and nucleated iPP. The dependence of the crystallization peak temperatures on the concentrations of Adi-Zn is shown in Figure 8. The peak crystallization temperature of iPP/Adi-Zn increased from 121 °C to approximately 124 °C with the addition of 0.025 wt % Adi-Zn and then slightly increased when the concentration was increased to 0.2 wt %. The peak crystallization temperature then remained relatively constant at higher Adi-Zn contents. These results indicate that Adi-Zn accelerated the crystallization of iPP at a very low additive concentration. The saturation concentration was approximately 0.2 wt %, which is in agreement with the results of impact strength tests.

The crystallization behavior of iPP/Adi-Zn was also investigated using POM, which allowed for direct observation of the crystallization process and crystal morphology of the polymer. Figure 9 shows photomicrographs of neat iPP and iPP with different amounts of Adi-Zn and with crystallization at 140 °C. In particular, the resulting morphology strongly depended on the amount of Adi-Zn. The spherulite sizes of iPP gradually decreased as the Adi-Zn concentration was increased to 0.2 wt %. The spherulite sizes barely changed for samples with an Adi-Zn content that exceeded 0.2 wt %, consistent with the DSC results. At low Adi-Zn concentrations, bright and colored β-spherulites were observed [indicated by the arrows in Figure 9(b)]. These results reveal that the β-NA (Adi-Zn) affected both the morphology and the crystal form of iPP.

CONCLUSIONS

A highly active and selective β-NA for iPP (zinc adipate, Adi-Zn) was developed. The effects of Adi-Zn on the mechanical properties and the β-crystal content of nucleated iPP were investigated. The impact strength of iPP nucleated with 0.2 wt % Adi-Zn was 1.8 times higher than that of neat iPP. In addition, WAXD analysis indicated that the content of β-crystals of nucleated iPP (k_β value) nearly exceeded 0.90 in an Adi-Zn concentration range from 0.025 to 1 wt %. A maximum k_β value of 0.973 was obtained at 0.1 wt % Adi-Zn, indicating that Adi-Zn is a highly active and selective β-NA for iPP. Furthermore, FSC studies using cooling rates of 60 to 13,800 °C min^{-1} revealed that the

formation of β-crystals significantly depended on the cooling rates. At cooling rates less than 3000 °C min^{-1}, only β-crystals were formed. However, at rates greater than 6000 °C min^{-1}, β-crystals failed to form. β- and α-crystals coexisted at cooling rates between 3000 and 6000 °C min^{-1}. Moreover, a lower critical crystallization temperature of approximately 100 °C, which corresponds to the generation of β-crystals, was investigated using cooling-induced crystallization; the results were in good agreement with those from a previous study.

ACKNOWLEDGMENTS

The authors gratefully acknowledge the National Natural Science Foundation of China (Grants 21476085) for financial support.

REFERENCES

1. Padden, F. J.; Keith, H. D. *J. Appl. Phys.* **1959**, *30*, 1479.
2. Meille, S. V.; Ferro, D. R.; Brückner, S.; Lovinger, A. J.; Padden, F. J. *Macromolecules* **1994**, *27*, 2615.
3. Karger-Kocsis, J. Polypropylene: Structure, Blends and Composites; Chapmann & Hall: London, **1995**, 50–94.
4. Moore, E. P. Polypropylene Handbook: Polymerization, Characterization, Properties, Processing, Applications, Hanser/Gardner Publications: Cincinnati, **1996**; p 113.
5. Varga, J. *J. Macromol. Sci.-Phys. B* **2002**, *41*, 1121.
6. Papageorgiou, D. G.; Chrissafis, K.; Bikiaris, D. N. *Polym. Rev.* **2015**, *55*, 596.
7. Luo, F.; Geng, C. Z.; Wang, K.; Deng, H.; Chen, F.; Fu, Q. *Macromolecules* **2009**, *42*, 9325.
8. Luijsterburg, B.; Jobse, P.; Merino, D. H.; Peijs, T.; Goossens, H. *J. Polym. Sci., Polym. Phys.* **2014**, *52*, 1071.
9. Chen, H. B.; Karger-Kocsis, J.; Wu, J. S.; Varga, J. *Polymer* **2002**, *43*, 6505.
10. Zhao, S. C.; Xin, Z. *Polymer* **2008**, *49*, 2745.
11. Varga, J. *Macromol. Sci. Phys.* **2002**, *B41*, 1121.
12. Su, Z. Q.; Dong, M.; Guo, Z. X.; Yu, J. *Macromolecules* **2007**, *40*, 4217.
13. Leugering, H. J. *Macromol. Chem.* **1967**, *109*, 204.
14. Shi, G.; Zhang, X.; Qiu, Z. *Macromol. Chem.* **1992**, *193*, 583.
15. Varga, J.; Mudra, I.; Ehrenstein, G. W. *J. Appl. Polym. Sci.* **1999**, *74*, 2357.
16. Li, X.; Hu, K.; Li, M.; Huang, Y.; Zhou, G. *J. Appl. Polym. Sci.* **2002**, *86*, 633.
17. Huo, H.; Jiang, S. C.; An, L. J.; Feng, J. C. *Macromolecules* **2004**, *37*, 2478.
18. Ikeda, N.; Kobayashi, T.; Killough, L. Polypropylene 96. World Congress: Zurich, Switzerland, September 18–20, **1996**.
19. Varga, J.; Menyhárd, A. *Macromolecules* **2007**, *40*, 2422.
20. Varga, J. In Polypropylene: Structure, Blends and Composites; Karger-Kocsis, J., Ed.; Chapmann & Hall: London, **1995**; Vol. *1*, p 56.
21. Krache, R.; Benavente, R.; López-Majada, J. M.; Pereña, J. M.; Cerrada, M. L.; Pérez, E. *Macromolecules* **2007**, *40*, 6871.
22. Chvátalová, L.; Navrátilová, J.; Čermák, R.; Raab, M.; Obadal, M. *Macromolecules* **2009**, *42*, 7413.
23. Bai, H. W.; Wang, Y.; Zhang, Z. J.; Han, L.; Li, Y. L.; Liu, L.; Zhou, Z. W.; Men, Y. F. *Macromolecules* **2009**, *42*, 6647.
24. Varga, J.; Fujiwara, Y.; Ille, A. *Chem. Eng.* **1990**, *34*, 255.
25. Lotz, B.; Fillon, B.; Thierry, A.; Wittmann, J. C. *Polym. Bull.* **1991**, *25*, 101.
26. Herwaarden, S.; Iervolino, E.; Herwaarden, F.; Wijffels, T.; Leenaers, A.; Mathot, V. *Thermochim. Acta* **2011**, *522*, 46.
27. Mathota, V.; Pydaa, M.; Pijpers, T.; Poel, G. V.; Kerkhof, E.; Herwaarden, S.; Herwaarden, F.; Leenaers, A. *Thermochim. Acta* **2011**, *522*, 36.
28. Androsch, R.; Monami, A.; Kucera, J. *J. Cryst. Growth* **2014**, *408*, 91.
29. Mollova, A.; Androsch, R.; Mileva, D.; Gahleitner, M.; Funari, S. S. *Eur. Polym. J.* **2013**, *49*, 1057.
30. Wang, J. T.; Shu, D.; Xiao, M.; Meng, Y. Z. *J. Appl. Polym. Sci.* **2006**, *99*, 200.
31. Sun, J. T.; Yuan, L. J.; Zhang, K. L.; Wang, D. L. *Thermochim. Acta* **2000**, *343*, 105.
32. Turner-Jones, A.; Aizlewood, J. M.; Beckett, D. R. *Makromol. Chem.* **1964**, *75*, 134.
33. Liu, M. X.; Guo, B. C.; Du, M. L.; Chen, F.; Jia, D. M. *Polymer* **2009**, *50*, 3022.
34. Zhao, S. C.; Xin, Z. *J. Polym. Sci. Polym. Phys.* **2010**, *48*, 653.
35. Kang, J.; He, J. H.; Chen, Z. F.; Yang, F.; Chen, J. Y.; Cao, Y.; Xiang, M. *Polym. Adv. Technol.* **2015**, *26*, 32.
36. Felice, D. S.; Sergey, A.; Giuseppe, T.; Christoph, S. *Macromolecules* **2006**, *39*, 2562.
37. Varga, J. *J. Therm. Anal. Calorim.* **1989**, *35*, 1891.
38. Mohmeyer, N.; Schmidt, H. W.; Kristiansen, P. M.; Altsädt, V. *Macromolecules* **2006**, *39*, 5760.

SGML and CITI Use Only
DO NOT PRINT